

# Liquid dynamics in partially crystalline glycerol

Alejandro Sanz\* and Kristine Niss

IMFUFA, Department of Science and Environment,  
Roskilde University, Postbox 260, DK-4000 Roskilde, Denmark

(Dated: September 27, 2018)

We present a dielectric study on the dynamics of supercooled glycerol during crystallization. We explore the transformation into a solid phase in real time by monitoring the temporal evolution of the amplitude of the dielectric signal. Neither the initial nucleation or the crystal growth influence the liquid dynamics visibly. For one of the samples studied, a tiny fraction of glycerol remained in the disordered state after the end of the transition. We examined the nature of the  $\alpha$  relaxation in this frustrated crystal and find that it is virtually identical to the bulk dynamics. In addition, we have found no evidence that supercooled glycerol transforms into a peculiar phase in which either a new solid amorphous state or nano-crystals dispersed in a liquid matrix are formed.

## I. INTRODUCTION

One of the longstanding questions in the field of condensed matter physics is what governs the liquid-to-glass transition and the concomitant dramatic slowing down of the transport quantities when supercooled liquids approach the glassy state on cooling<sup>1–3</sup>. At the glass transition temperature  $T_g$ , the liquid falls out of thermodynamic equilibrium because the molecular rearrangements become so slow that the equilibrium volume and enthalpy<sup>4,5</sup> cannot be reached on experimental time scales. In fact, the main focus in the field is the molecular relaxation taking place in the supercooled liquid just above  $T_g$ . The main relaxation process, referred to as the  $\alpha$  relaxation, is cooperative in nature and can be measured as a response to a wide range of external perturbations, for instance mechanical or electrical<sup>6</sup>. The glass-formers community has widely exploited the imaginary part of the complex dielectric permittivity because of its high sensitivity to external factors such as temperature and pressure, and also to microscopic properties of the substance such as its degree of order, physical interactions with the surroundings, and geometrical confinement among others<sup>7–13</sup>.

Glycerol (propane-1,2,3-triol) is one of the most studied molecular glass-formers, principally for its extremely low tendency to crystallize<sup>14–20</sup>. Since glycerol normally forms a highly stable supercooled liquid (large viscosity upon melting<sup>17</sup>), little attention has been paid to its crystalline phase. Even so, one can find in the literature several works mainly focused on the high frequency dynamics of the crystalline state<sup>21–23</sup>. Nevertheless, real time investigations of its transformation into solid-like structures have recently attracted the interest of some authors<sup>24,25</sup>. Inspired by previous works on the existence of long-lived dynamic heterogeneities in supercooled glycerol, Möbius *et al.* performed real time aging experiments above  $T_g$  and detected the formation of a solid phase that showed a distinct mechanical response as compared to the orthorhombic crystal<sup>24</sup>. This solid-like phase presented a value of the shear modulus two orders of magnitude lower than that of standard crystalline glycerol. In this way, Möbius and co-authors *speculated*

on the existence of a glacial phase<sup>26</sup>, that is, either a second amorphous state or a frustrated crystal with a high degree of defects and disorder. Two years later, by employing time-resolved neutron scattering, Yuan and co-authors aimed to unravel the structural nature of this solid-like phase<sup>25</sup>. They revealed, in agreement with one of the interpretations given by Möbius *et al.*, the formation of a crystalline lattice.

It is well established that there is an interplay between structure and dynamics on the phenomenon of crystallization<sup>27–31</sup>, though the exact nature of this is not fully understood. The focus in this paper is on how the nucleation and growth steps of crystallization of glycerol affect the dynamics of the remaining liquid. Moreover we study the dynamics of a partially disordered sample, inquiring about the putative existence of a glacial phase.

## II. SAMPLE PREPARATION AND EXPERIMENTAL TOOLS

Anhydrous glycerol ( $\geq 99.5\%$  purity, Sigma-Aldrich<sup>®</sup>) was used without additional purification and was manipulated, as much as we could, under nitrogen to avoid the uptake of ambient water. In order to carry out the present study, we utilized dielectric spectroscopy, using a sample cell especially designed for this kind of measurement. It consists of two parallel metal plates separated by a Kapton<sup>®</sup> spacer of 0.25 mm thickness. With the purpose of insulating the sample cell electrically and also from possible water contamination, the capacitor was sealed by means of a cylindrical container made of polyether ether ketone (*PEEK*).

We filled the transducer with dry glycerol under nitrogen flow inside a glove bag. Once the cell was properly closed, it was transferred to the measuring cryostat. For a detailed description of the dielectric spectroscopy set-up and sample environment control we refer the reader to the following publication<sup>32,33</sup>.

The standard procedure we followed to induce the crystallization of supercooled glycerol consisted of the thermal protocol described in Fig. 1. We cooled down the sample from 300 K to 190 K at a cooling rate of ap-

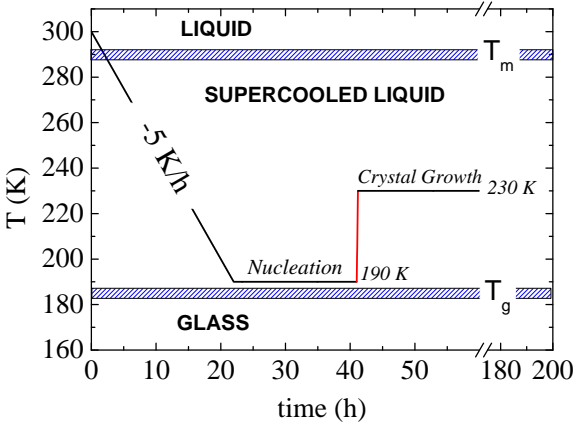


FIG. 1. Thermal protocol for inducing the transformation of liquid glycerol into the crystalline phase. Nucleation of crystalline seeds is promoted by annealing at 190 K during 19 hours. Crystal growth takes place at 230 K after fast heating from 190 K.

proximately 5 K/h. Then, an isothermal annealing at 190 K was carried out. Finally, we heated up to 230 K where we monitored isothermally the dielectric signal as crystallization occurred.

### III. RESULTS

#### A. Dynamics of the fully disordered liquid

First, we examined the dynamics of the fully disordered liquid between 195 and 240 K on heating. We explored the  $\alpha$  relaxation by measuring the frequency evolution of the complex dielectric permittivity,  $\varepsilon^*(\omega) = \varepsilon'(\omega) - i\varepsilon''(\omega)$ , where  $\omega$  is the angular frequency, and  $\varepsilon'$  and  $\varepsilon''$  are the real and imaginary parts respectively, which were in agreement with the literature<sup>16,19</sup>. We described the relaxation curves with a dielectric version of the  $\alpha$  circuit model, also known as the dielectric version of the Extended Bell (EB) model<sup>34</sup>. The complex dielectric permittivity according to the  $\alpha$  circuit model reads as follows:

$$\varepsilon^*(\omega) = \varepsilon_\infty + \frac{\Delta\varepsilon}{1 + \frac{1}{(i\omega\tau_\alpha)^{-1} + k_\alpha(i\omega\tau_\alpha)^{-\alpha}}} \quad (1)$$

Here,  $\varepsilon_\infty$  is the instantaneous or unrelaxed dielectric constant,  $\Delta\varepsilon$  is the dielectric strength,  $\tau_\alpha$  is the  $\alpha$ -relaxation time,  $\alpha$  is the high-frequency power law<sup>35</sup> and  $k_\alpha$  determines the broadening of the  $\alpha$  peak.

#### B. Dynamics during nucleation

The main aim of this work is to explore the dynamics-structure relationships during the transformation of liq-

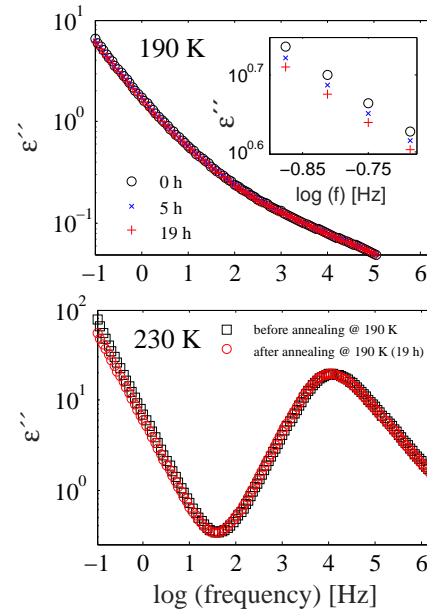


FIG. 2. (Top) Frequency dependence of the imaginary part of the complex dielectric permittivity in glycerol during isothermal annealing at 190 K. The inset zooms the low frequency flank of the dielectric loss for a more detailed examination. (Bottom) Dielectric spectra of glycerol collected at 230 K, first by cooling from room temperature and second after annealing at 190 K.

uid glycerol into a solid phase. A fresh sample was thus subjected to the thermal protocol displayed in Fig. 1. It has been reported that the formation of ordered solid phases in glycerol is favored by a slow cooling to temperatures slightly above  $T_g$ <sup>24</sup>, followed by two successive isothermal treatments for triggering nucleation and crystal growth respectively. In order to demonstrate the formation of crystals seeds during the thermal treatment at 190 K, selected measurements at this temperature and comparisons of the spectra at 230 K before and after such nucleation are presented in Fig. 2(top) and Fig. 2(bottom) respectively. During nucleation, there is a slight decrease of the permittivity. Whether this reduction is a consequence of changes at the molecular level associated with crystal nucleation or simply slow geometrical adjustments of the capacitor due to mismatch of sample and spacer thermal-expansion coefficients is hard to elucidate. Nevertheless, the bottom panel of Fig. 2 proves the sample did not undergo any kind of crystal growth at 190 K as indicated by the almost identical spectrum before and after such nucleation period.

In Fig. 3 we show the kinetics of crystallization at 230 K for different nucleation conditions. The non-annealed sample was directly cooled from room temperature to 230 K at a cooling rate of 5 K/h. The data in Fig. 3 indicate that crystal growth becomes faster with longer periods of annealing at 190 K. This finding implies the formation of

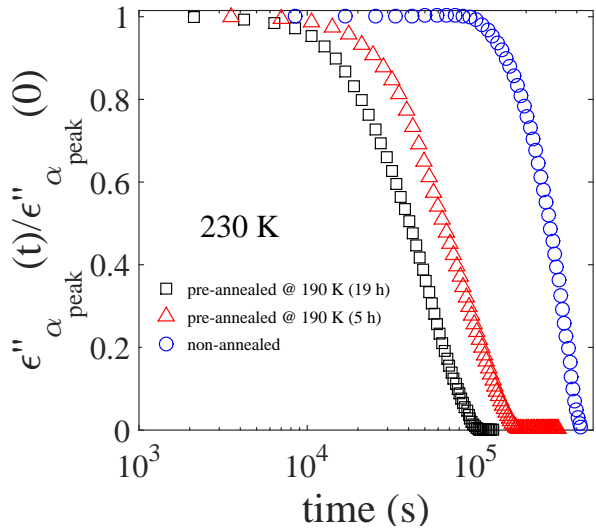


FIG. 3. Time evolution of the maximum intensity of the loss peak upon crystallization at 230 K for samples without annealing (blue circles) or with annealing at 190 K during 5 h (red triangles) or for 19 h (black squares). Data are normalized to the initial value.

crystalline nuclei at 190 K which subsequently organize into the crystal lattice at 230 K. We interpret this as an indication that there is in fact a structural difference between samples before and after annealing at 190 K. The fact that the two dielectric signals are identical tells us that the formation of nuclei is a very local process that does not have any global effect on the liquid dynamics.

### C. Liquid dynamics during crystal growth

With the purpose of studying the influence of crystallization on the cooperative dynamics in glycerol, frequency sweeps from 100 mHz to 1 MHz (total acquisition time 11.7 min.) were collected continuously at a constant temperature of 230 K. Selected snapshots of this real time investigation are presented in Fig. 4. The dielectric relaxation response remains unchanged during the early stages, but its intensity starts to monotonically decrease after an induction period and finally the  $\alpha$  relaxation peak totally vanishes. According to the theory of dielectric relaxation and ignoring possible variations of the dipole-dipole correlations, we may consider the following proportionality

$$\Delta\epsilon \propto \frac{\mu^2 N}{k_b T} \quad (2)$$

where  $\mu$  is the molecular dipole moment,  $k_b$  is the Boltzmann constant,  $T$  is the temperature and  $N$  corresponds to the total number of reorientating dipoles in the system<sup>36</sup>. Assuming that the transformation of a liquid substance into a crystal carries with it the corresponding

reduction of  $N$  fluctuating species as molecules abandon the disordered phase and attach to the surface of growing crystals, where molecules become translational and rotationally immobile, one accordingly expects a depletion of  $\Delta\epsilon$  via Eq. 2. This effect is clearly observed in both components of the complex permittivity as displayed in Fig. 4. The low frequency dispersion detected in  $\epsilon''(\omega)$ , which is assigned to pure ohmic conduction, decreases approximately at the same rate as the  $\alpha$  relaxation peak. A reduction of the dc conductivity upon crystallization is in agreement with arguments that inversely correlate the conduction of free charges with the viscosity of the medium according to the Debye-Stokes-Einstein relation<sup>37</sup>. It is important to remark that crystalline glycerol shows a shear viscosity larger than the one for the supercooled liquid<sup>24</sup>. Therefore we expect a larger viscosity for the composite material as crystallization proceeds. This would explain why the dc-conductivity decreases in spite of the  $\alpha$  relaxation time remains unchanged. Besides, there is a significant modification of the charge-transport mechanism as revealed by the onset of a sublinear power law at low frequencies as crystallization proceeds. A detailed discussion of this crossover is beyond the scope of the present manuscript, but it deserves more attention in the future. Apart from the total extinction of the structural relaxation when the crystallization ended, it is important to remark that the location of the peak remained unchanged during the whole process, suggesting that the intrinsic nature of the structural relaxation of glycerol remains unaltered in the course of crystallization. A more detailed work on the temperature dependence of the kinetics of crystallization has also been carried out and it will be the subject of a future publication<sup>38</sup>. We have also considered possible Maxwell-Wagner-type<sup>39</sup> effects on the dielectric signal.

### D. Liquid dynamics after aborted crystallization

We explored the crystallization of glycerol at different temperatures several times. In one single case, the ordering process did not proceed to the end, and a small fraction of liquid phase ( $\sim 1\%$ ) got trapped between the crystalline domains. To illustrate this aborted crystallization, Fig. 5(top) shows the evolution of the  $\alpha$  relaxation as a function of crystallization time. Contrary to the data set shown in Fig. 4, a residual and stable  $\alpha$  peak is still detected once the crystallization terminates. Such coexistence between crystallites and disordered domains giving rise to an  $\alpha$  peak is a well-known and general phenomenon in the field of semi-crystalline polymers<sup>9</sup>. Here, the stability of this residual relaxation was confirmed over more than 24 hours without any indication of losing intensity, broadening or shifting in frequency.

The kinetics of crystallization was evaluated by calculating the volume fraction of the new phase at different crystallization times  $N(t)$  from the maximum intensity of the loss peak by means of the following expression:

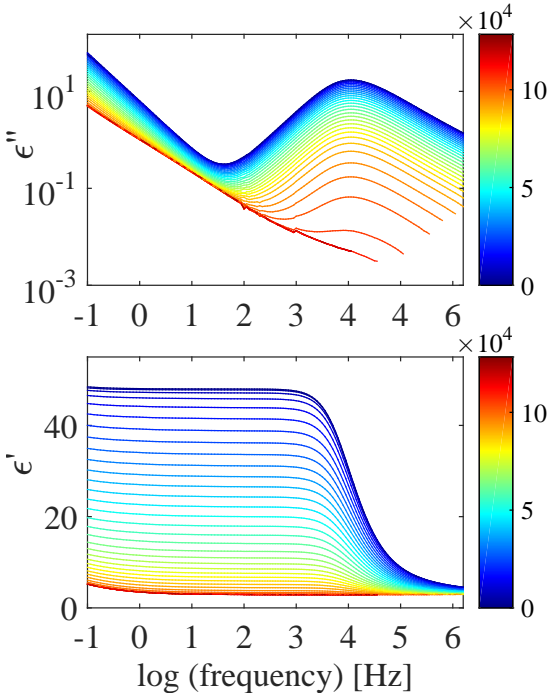


FIG. 4. Complex dielectric permittivity of supercooled glycerol upon crystallization at 230 K. Imaginary (top) and real part of the permittivity (bottom) are represented as a function of frequency at different stages of crystallization. Colorbars indicate the crystallization time in seconds.

$$N(t) = \frac{\varepsilon''_{\alpha_{peak}}(0) - \varepsilon''_{\alpha_{peak}}(t)}{\varepsilon''_{\alpha_{peak}}(0) - \varepsilon''_{\alpha_{peak}}(\infty)} \quad (3)$$

where  $\varepsilon''_{\alpha_{peak}}(0)$  is the value of the dielectric loss at the frequency where the  $\alpha$  peak is located ( $\log(f) = 4.05$  Hz) for the pure liquid,  $\varepsilon''_{\alpha_{peak}}(t)$  takes the corresponding values at different crystallization times and  $\varepsilon''_{\alpha_{peak}}(\infty)$  corresponds to the value of the dielectric loss at the same frequency for the pure crystal. For the specific case where the crystallization stopped and the exact value of  $\varepsilon''_{\alpha_{peak}}(\infty)$  is unknown, we assume the same ratio between  $\varepsilon''_{\alpha_{peak}}(0)$  and  $\varepsilon''_{\alpha_{peak}}(\infty)$  obtained for the data at 230 K shown in Fig. 4.

Figure 5 (bottom) shows the time evolution of  $N(t)$  during isothermal treatment at 230 K for the complete (red squares) and aborted (black circles) phase transformations. In both cases,  $N(t)$  follows a sigmoidal fashion in accordance with previous studies on crystalline growth<sup>27</sup>. In general terms, the kinetics of the transitions are quite similar, and one only detects significant differences close to the end where the maximum value of the volume fraction of the new phase does not reach 1 in one of the cases.

With the purpose of elucidating the dynamic properties of the liquid phase in the frustrated crystal, the

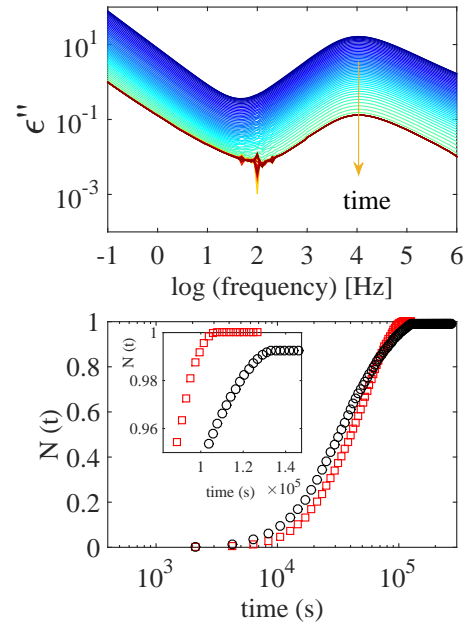


FIG. 5. (Top) Dielectric loss in logarithmic scale of the  $\alpha$  relaxation as a function of frequency at different crystallization times during isothermal annealing at 230 K. Snapshots are shown every  $3.5 \times 10^3$  s during a total crystallization time of  $2.7 \times 10^5$  s. (Bottom) Time dependence of the crystalline volume fraction at 230 K for the complete (red squares) and aborted (black circles) crystallization processes. The inset zooms the late stages to highlight the frustrated crystallization shown in the top panel.

sample described in Fig. 5(top) was subsequently cooled down to temperatures just above  $T_g$ , collecting isothermally every 5 K the frequency dependence of the complex permittivity.

Full lines in Fig. 6 correspond to the fit of the experimental data to the EB or  $\alpha$ -circuit model (Eq. 1). In both cases, the values of  $\alpha$  were set to 0.5 for the whole temperature range. Since we were just interested in the  $\alpha$  peak and due to the limited frequency range, the slight increase of dispersion at the high frequency flank of the  $\alpha$  peak, the so-called excess wing, was not taken into consideration<sup>16</sup>.

A close comparison of the fitting parameters of Eq. 1 for the liquid and aborted crystalline samples is shown in Fig. 7. Regarding the broadening parameter  $k_\alpha$ , Fig. 7(c) presents a similar behaviour for both kind of liquids. The values of  $k_\alpha$  increase when temperature decreases which indicates a broader width of the distribution of relaxation times when approaching  $T_g$ <sup>16</sup>. The values of  $k_\alpha$  account for the departure of the relaxation width from the simplest Debye model in such a way that large values of  $k_\alpha$  will lead to a less Debye-like relaxation<sup>34,40</sup>. For the frustrated crystal one may observe slightly higher values. It is tempting to correlate this increase of  $k_\alpha$  with a more heterogeneous landscape. However, the difference is not very prominent and we have to take into consideration

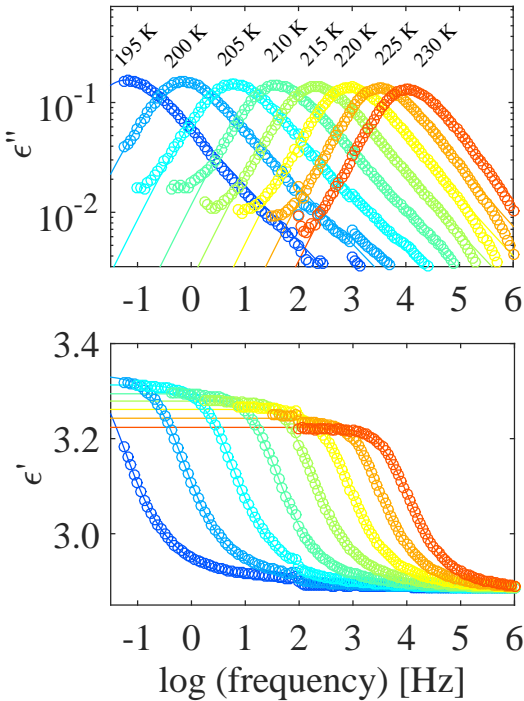


FIG. 6. Dielectric spectra of residual liquid glycerol in a frustrated crystalline phase at the labelled temperatures. Continuous lines represent the best fit of the experimental data to the EB model.

that the amplitude of the relaxation for the frustrated crystal is very low, which means that the curve shape is also determined with less precision. The evolution of  $\Delta\epsilon$  with temperature shows a similar trend for the liquid and frustrated crystal. In both cases,  $\Delta\epsilon$  decreases with temperature in qualitative agreement with previous reports on supercooled glycerol<sup>16</sup>.

In Fig. 7(d) we have plotted the characteristic relaxation times of the  $\alpha$  process in the Arrhenius representation. As expected, the temperature dependence of the  $\alpha$  relaxation times deviates from linearity as temperature goes down. For both types of liquid glycerol, the values of  $\tau_\alpha$  can be described by the empirical Vogel-Fulcher-Tamman (VFT) relation:

$$\tau_\alpha = \tau_0 \exp\left(\frac{DT_0}{T - T_0}\right) \quad (4)$$

where  $\tau_0$  is a pre-exponential factor with phonon-like time scales,  $D$  is a strength parameter related to the dynamic fragility through the following expression  $m=16+590/D$  and  $T_0$  is the Vogel temperature ( $T_0 < T_g$ )<sup>41</sup>. Leaving aside the physical meaning of the parameters in Eq. 4 (see eg.<sup>42</sup> for a discussion), the usefulness of the VFT law for interpolating experimental points and quantifying the steepness of the relaxation plot is widely accepted<sup>1,2,4,42</sup>. Solid lines in Fig. 7(d) correspond to the fits of the data to the VFT equation for the pure liq-

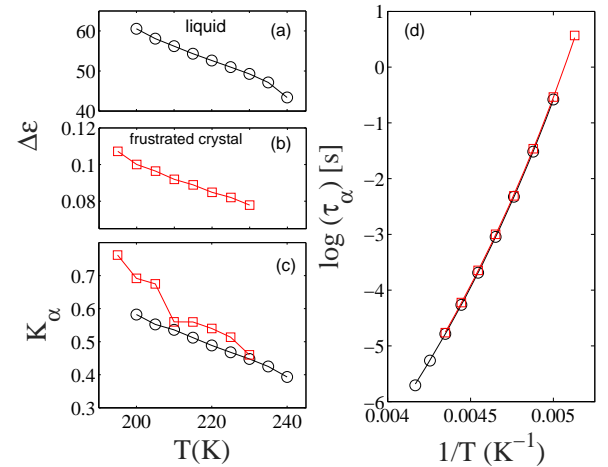


FIG. 7. Temperature dependence of the fitting parameters of the EB model (Eq. 1) for the pure liquid (black circles) and frustrated crystalline glycerol (red squares). Panels *a* and *b* display the dielectric strength  $\Delta\epsilon$  and panel *c* the broadening parameter  $k_\alpha$ . In panel *d* we show the characteristic relaxation times of the  $\alpha$  process with reciprocal temperature. Solid lines in *d* are fits to the VFT equation. Lines in *a*, *b* and *c* are guides to the eye.

TABLE I. VFT parameters of the  $\alpha$  process for the pure liquid and for the remaining liquid fraction embedded in the frustrated crystal.

VFT Parameter	Pure Liquid	Frustrated Crystal
$\log \tau_0$ (s)	-14.8	-14.9
D	18.3	18.6
$T_0$ (K)	128	128

uid and frustrated crystalline samples. For consistency, the relaxation times for the two kinds of liquids were fitted in the same temperature range (200-230 K). Both the data and the VFT lines practically overlap, which indicates that the nature of the  $\alpha$  relaxation dynamics is not significantly altered by the presence of crystals. Similar values of the VFT parameters to those collected here in Table I have been reported in the literature<sup>16,43</sup>.

#### IV. DISCUSSION

We have explored the formation of solid structures in real time in the well-known glass former glycerol. The solidification was induced by a two-step annealing procedure as suggested before<sup>24,25</sup>. Our dielectric data reveal that liquid glycerol, through a nucleation step at 190 K and subsequent crystal growth at 230 K, transforms into a new phase. In most cases (not all of them shown here<sup>38</sup>), we have found a total disappearance of the  $\alpha$  relaxation, a fact which suggests that glycerol transforms into the standard orthorhombic crystalline phase<sup>21</sup>. The fact that in one of the samples studied here (Fig. 5)

the end of the crystallization was suddenly aborted could explain prior results that speculated the formation of a glacial phase in which metastable nano-crystals were embedded in a liquid matrix<sup>18,24,25</sup>. Our data just show an unfinished ordering process that resulted in a small fraction of sample remaining in the liquid state. Unlike in polymeric materials where the formation of semi-crystalline structures is a common feature, few examples can be found in the literature of a low molecular weight liquid that does not crystallize into a 100 % crystalline system<sup>27</sup>.

We have presented evidence that the nature of the  $\alpha$  relaxation dynamics does not undergo important modifications during crystallization. We have extended our study along the whole crystallization process, from a well controlled nucleation step to the crystal growth. Interestingly, the structural relaxation remained unaffected, first by the density fluctuations that trigger the formation of nuclei, and second during the thickening of the lattice structure.

Taking advantage to the aborted crystallization that took place in one of the studied samples, we could explore the temperature evolution of the  $\alpha$  relaxation associated with a small fraction of liquid phase surrounded by the crystalline network. Our results indicate that the dynamics remained virtually identical to the bulk liquid in terms of location of the  $\alpha$  peak, spectral shape and activation energy. A relaxation process in crystalline glycerol was reported by Ryabov *et al.*<sup>44</sup>, where a sample of dry glycerol was crystallized on heating, giving as a result a new dielectric mode five orders of magnitude slower than the  $\alpha$  process for the pure liquid. This new mode exhibited an Arrhenius behaviour, similar to other dielectric relaxation processes detected in molecular crystals,<sup>45,46</sup> and it was assigned by the authors to either defects in the crystalline lattice or to the presence of disordered domains located at the interface between crystalline grains. In contrast to the observation by Ryabov *et al.*<sup>44</sup>, here we detect a relaxation with the same features as the one showed by the pure liquid, in such a way that we may confirm that it does not correspond to the relaxation of crystalline glycerol itself, but to a kind of metastable semi-crystalline system. We do not see any evidence of the slow mode reported by Ryabov *et al.*<sup>44</sup>.

Several factors have been proposed to affect the mobility of the liquid at the proximities of the crystal/liquid interfaces during crystallization, including the existence of pre-ordered configurations and the different ability of the molecules to be accommodated on the surface of the growing lattice<sup>27</sup>. In the latter case, it is expected that not all molecules near the crystal/liquid interface show the same geometrical preferences to attach to the crystal. For both cases, the activation energy that governs diffusion over short distances may increase as compared to the pure liquid<sup>27</sup>. Here we report that glycerol, at least for the time scale detected by dielectric spectroscopy, does not present variations in its mobility upon crystalliza-

tion.

The molecules in crystalline glycerol are in an extended conformation in which the two dihedral angles defined by the intersection between two specified planes within the molecule are situated in a range of 120° and 240°<sup>21</sup>. On the contrary, Towey *et al.*<sup>47</sup> have recently reported that in the liquid state the most probable conformer shows a less extended structure in which the second dihedral angle presents values in the range 240-360°. Therefore, the transference of units from the liquid on to the surface of the growing crystal should imply, at least for an important fraction of molecules, the necessity of conformational transitions to the extended or coplanar configuration. However, according to our data, this does not cause any global effect on the dynamics. The lack of dynamical signature of the crystallization process indicates that the changes in the hydrogen bonding network as well as the conformational changes taken place during the crystallization are very local. Thus, very few molecules at the phase boundary are changing structure while the majority of the molecules are either in the crystal or in the ordinary bulk liquid.

## V. CONCLUSIONS

We present, to the best of our knowledge, the first study in real time of the isothermal crystallization of glycerol by using dielectric spectroscopy. We demonstrate that liquid glycerol transforms into a crystalline material by following a two-step nucleation and crystal growth protocol. Our results do not support the formation of a distinct solid phase from the standard crystalline lattice. We have also shown that in one of the samples studied, the starting liquid transformed into an incomplete crystalline phase with a residual liquid fraction. For a period of more than one day we proved the metastability of this frustrated crystal. The dynamics of this remaining liquid phase were studied as a function of temperature showing features very close to the pure liquid material. In addition to that, we have shown that during the ordering process the  $\alpha$  relaxation dynamics remains unaltered, revealing that neither the nucleation period nor the crystal growth affected the nature of the cooperative motions in supercooled glycerol.

## ACKNOWLEDGMENTS

This work has been funded by the Danish Council for Independent Research (Sapere Aude: Starting Grant). Technical support from the workshop at IMFUFA (Department of Science and Environment, Roskilde University) is acknowledged. We also thank Michael Greenfield for technical support.

- \* asanz@ruc.dk
- <sup>1</sup> P. Debenedetti and F. Stillinger, *Nature* **410**, 259 (2001).
- <sup>2</sup> L. Berthier and G. Biroli, *Reviews of Modern Physics* **83**, 587 (2011).
- <sup>3</sup> L. Berthier and M. D. Ediger, *Physics Today* **69**(1), 40 (2016).
- <sup>4</sup> M. Ediger, C. Angell, and S. Nagel, *Journal of Physical Chemistry* **100**, 13200 (1996).
- <sup>5</sup> J. C. Dyre, *Journal of Physics: Condensed Matter* **19**, 205105 (2007).
- <sup>6</sup> B. Jakobsen, C. Maggi, T. Christensen, and J. C. Dyre, *Journal of Chemical Physics* **129**, 184502 (2008).
- <sup>7</sup> P. Sillren, A. Matic, M. Karlsson, M. Koza, M. Maccarini, P. Fouquet, M. Goetz, T. Bauer, R. Gulich, P. Lunkenheimer, A. Loidl, J. Mattsson, C. Gainaru, E. Vynokur, S. Schildmann, S. Bauer, and R. Böhmer, *Journal of Chemical Physics* **140**, 124501 (2014).
- <sup>8</sup> M. Paluch, M. Sekula, S. Pawlus, S. Rzoska, J. Ziolo, and C. Roland, *Physical Review Letters* **90**, 175702 (2003).
- <sup>9</sup> A. Nogales, Z. Denchev, I. Sics, and T. Ezquerra, *Macromolecules* **33**, 9367 (2000).
- <sup>10</sup> K. Murata and H. Tanaka, *Nature Materials* **11**, 436 (2012).
- <sup>11</sup> P. Lunkenheimer, R. Wehn, and A. Loidl, *Journal of Non-Crystalline Solids* **352**, 4941 (2006).
- <sup>12</sup> J. Martin, C. Mijangos, A. Sanz, T. A. Ezquerra, and A. Nogales, *Macromolecules* **42**, 5395 (2009).
- <sup>13</sup> M. Arndt, R. Stannarius, H. Groothues, E. Hempel, and F. Kremer, *Physical Review Letters* **79**, 2077 (1997).
- <sup>14</sup> J. Wuttke, J. Hernandez, G. Li, G. Coddens, H. Z. Cummins, F. Fujara, W. Petry, and H. Sillescu, *Physical Review Letters* **72**, 3052 (1994).
- <sup>15</sup> P. Lunkenheimer, A. Pimenov, M. Dressel, Y. Goncharov, R. Bömer, and A. Loidl, *Physical Review Letters* **77**, 318 (1996).
- <sup>16</sup> P. Lunkenheimer and A. Loidl, *Chemical Physics* **284**, 205 (2002).
- <sup>17</sup> K. Schröter and E. Donth, *The Journal of Chemical Physics* **113**, 9101 (2000).
- <sup>18</sup> R. Zondervan, T. Xia, H. van der Meer, C. Storm, F. Kulzer, W. van Saarloos, and M. Orrit, *Proceedings of the National Academy of Sciences of the United States of America* **105**, 4993 (2008).
- <sup>19</sup> Y. Hayashi, A. Puzenko, and Y. Feldman, *Journal of Non-Crystalline Solids* **352**, 4696 (2006).
- <sup>20</sup> L. A. Roed, D. Gundermann, J. C. Dyre, and K. Niss, *Journal of Chemical Physics* **139**, 101101 (2013).
- <sup>21</sup> F. J. Bermejo, A. Criado, A. de Andres, E. Enciso, and H. Schober, *Physical Review B* **53**, 5259 (1996).
- <sup>22</sup> C. Talon, Q. Zou, M. Ramos, R. Villar, and S. Vieira, *Physical Review B* **65**, 012203 (2001).
- <sup>23</sup> U. Buchenau, R. Zorn, and M. A. Ramos, *Physical Review E* **90**, 042312 (2014).
- <sup>24</sup> M. E. Möbius, T. Xia, W. van Saarloos, M. Orrit, and M. van Hecke, *The Journal of Physical Chemistry B* **114**, 7439 (2010).
- <sup>25</sup> H.-F. Yuan, T. Xia, M. Plazanet, B. Dem, and M. Orrit, *Journal of Chemical Physics* **136**, 041102 (2012).
- <sup>26</sup> A. Ha, I. Cohen, X. Zhao, M. Lee, and D. Kivelson, *The Journal of Physical Chemistry* **100**, 1 (1996).
- <sup>27</sup> M. Descamps and E. Dudognon, *Journal of Pharmaceutical Sciences* **103**, 2615 (2014).
- <sup>28</sup> K. Adrjanowicz, K. Kaminski, M. Paluch, and K. Niss, *Crystal Growth & Design* **15**, 3257 (2015).
- <sup>29</sup> P. Tripathi, M. Romanini, J. L. Tamarit, and R. Macovez, *International Journal of Pharmaceutics* **495**, 420 (2015).
- <sup>30</sup> A. Sanz, M. Jimenez-Ruiz, A. Nogales, D. Marero, and T. Ezquerra, *Physical Review Letters* **93**, 015503 (2004).
- <sup>31</sup> J. Dobbertin, J. Hannemann, C. Schick, M. Ptter, and H. Dehne, *The Journal of Chemical Physics* **108**, 9062 (1998).
- <sup>32</sup> B. Igarashi, T. Christensen, E. H. Larsen, N. B. Olsen, I. H. Pedersen, T. Rasmussen, and J. C. Dyre, *Review of Scientific Instruments* **79**, 045106 (2008).
- <sup>33</sup> B. Igarashi, T. Christensen, E. H. Larsen, N. B. Olsen, I. H. Pedersen, T. Rasmussen, and J. C. Dyre, *Review of Scientific Instruments* **79**, 045105 (2008).
- <sup>34</sup> N. Sağlanmak, A. I. Nielsen, N. B. Olsen, J. C. Dyre, and K. Niss, *The Journal of Chemical Physics* **132**, 024503 (2010).
- <sup>35</sup> It is well documented that the dielectric loss of the  $\alpha$  relaxation of viscous molecular liquids at the high frequency limit shows a power law dependence of  $\omega^{-\alpha}$ , where  $\alpha$  normally takes values of 0.5 when temperature approaches the glass transition.
- <sup>36</sup> A. Schönhals and F. Kremer, *Broadband Dielectric Spectroscopy*, Springer-Verlag Berlin Heidelberg (2003).
- <sup>37</sup> C. M. Roland, S. Hensel-Bielowka, M. Paluch, and R. Casalini, *Reports on Progress in Physics* **68**, 1405 (2005).
- <sup>38</sup> A. Sanz and K. Niss, unpublished.
- <sup>39</sup> M. H. Jensen, C. Alba-Simionescu, K. Niss, and T. Hecksher, *The Journal of Chemical Physics* **143**, 134501 (2015).
- <sup>40</sup> P. Debye and H. Falkenhagen, *Physikalische Zeitschrift* **29**, 401 (1928).
- <sup>41</sup> R. Böhmer, K. L. Ngai, C. A. Angell, and D. J. Plazek, *The Journal of Chemical Physics* **99**, 4201 (1993).
- <sup>42</sup> T. Hecksher, A. I. Nielsen, N. B. Olsen, and J. C. Dyre, *Nature Physics* **4**, 737 (2008).
- <sup>43</sup> S. Sudo, M. Shimomura, N. Shinyashiki, and S. Yagihara, *Journal of Non-Crystalline Solids* **307-310**, 356 (2002).
- <sup>44</sup> Y. Ryabov, Y. Hayashi, A. Gutina, and Y. Feldman, *Physical Review B* **67**, 132202 (2003).
- <sup>45</sup> A. Sanz, D. Rueda, A. Nogales, M. Jimenez-Ruiz, and T. Ezquerra, *Physica B: Condensed Matter* **370**, 22 (2005).
- <sup>46</sup> K. Amann-Winkel, C. Gainaru, P. H. Handle, M. Seidl, H. Nelson, R. Böhmer, and T. Loerting, *Proceedings of the National Academy of Sciences of the United States of America* **110**, 17720 (2013).
- <sup>47</sup> J. J. Towey, A. K. Soper, and L. Dougan, *Physical Chemistry Chemical Physics* **13**, 9397 (2011).